

1. CLIMATE AND ENVIRONMENTAL MODELLING

1.1 Climate Variabilities in the Tropics: Genesis and Simulation

The tropical climate is strongly modulated by a number of interannual variabilities like El-Nino Southern Oscillation (ENSO) and the Quasi-Biennial Oscillation (QBO). Although a large number of studies have addressed the questions of their genesis and structure, important conceptual issues remain. It is not clear, for example, if the ocean atmosphere coupling is necessary to excite them. Nor is the general mechanism that generates these low frequency climate variabilities clearly understood. These questions, on the other hand, lie at the centre of any attempt at understanding, simulation and long-term prediction of tropical climate. Using the C-MMACS Tropical Anomaly Climate (CTAC) model and observed data from the Comprehensive Ocean-Atmosphere Data Set (COADS), a large part of the tropical variabilities can be understood as responses to convective internal dynamics. Results from further investigation with CTAC model on the role of convective internal dynamics modulated by Sea Surface Temperature (SST) and mean surface winds in generating interannual variabilities with observed structures are reported here.

In the conventional dynamical scenario, these variabilities appear as responses to forcing induced by the ocean-atmosphere coupling. However, this issue is far from conclusive; while the ocean-atmosphere coupling is expected to play a significant role in long-period oscillations, the nature of forcing necessary for the genesis of these variabilities and, in particular, the role of an explicit ocean-atmosphere coupling remains unanswered.

A proper understanding of this issue can significantly contribute to the quality and range of long-term prediction and the nature of forcing necessary to generate these variabilities thus needs to be examined. Three questions stand out in particular:

- Is an explicit ocean-atmosphere coupling necessary for the genesis of ENSO-type variabilities?
- Can these climate variabilities be sustained by internal (convective) dynamics of the tropical atmosphere, and
- Is it at all necessary to invoke the observed interannual variability of SST (which essentially comes from an atmospheric forcing) to explain atmospheric interannual variabilities?

These three questions are addressed using a validated model for the low-level anomaly climate in the tropics. The dynamical scenario is that of the internal convective dynamics of a moist tropical atmosphere, characterized by a convective relaxation time scale (CRT) which governs the anomaly heating. The concept and the formulation of a CRT were discussed earlier, mostly in an analytical context. The basic philosophy is that 'organized' large-scale precipitation in the tropics has a characteristic relaxation time scale, typically of a few hours. The use of the concept of a CRT permits us to explore mechanisms different from those present in the conventional formulation of convective heating. The convective internal dynamics in this model is also modulated by (observed) SST and the surface winds.

A long-term simulation was generated by integrating

the model for thirty eight years with a given observed initial condition with mean fields and SST from the 38-year (1950-1987) COADS. It was found that a spatially and temporally uniform SST cannot generate the structure of the observed tropical variabilities (monthly mean structure of the anomaly fields) or the intra seasonal oscillation (ISO). On the other hand, with a CRT of about an hour and with a mean climatological annual cycle of SST, the model reproduces a large part of the observed structure of the anomaly fields as well as the structure of ISO. Thus, the subsequent experiments on interannual variabilities were carried out with a space-time dependent SST and a value of CRT equal to 0.5 hours. The characteristics of the ISO in the long-term simulations were then compared with those from the composite one-year simulations for cross-validating the two simulations with different mean fields, initial conditions and periods of integration. This cross validation allows a more objective evaluation of the model performance.

After validating the model, a number of long-term simulations were carried out to investigate the nature of interannual variabilities. To delineate the longer term oscillations with relatively weaker power than the annual oscillation, the time series were subjected to a 12-month running averaging. We present in the foregoing, the results from the following experiments designed to address the questions we have set forth:

- *Expt.A:* Observed interannual variability in both SST and the mean surface winds,
- *Expt.B:* Interannual variability only in the mean surface winds, with an observed climatological mean annual cycle of SST,
- *Expt.C:* Interannual variability only in the

mean surface winds, with interannual variability of SST only in the summer months (June, July and August),

- *Expt.D:* Interannual variability only in the mean surface winds, with interannual variability of SST only in the winter months (preceding December, January and February) and
- *Expt.E:* Climatological mean annual cycle of surface winds, with a random interannual variability (maximum amplitude 0.4) superimposed on the observed climatological mean annual cycle of SST.

To examine various periodicities, the time series of the model fields were subjected to a power spectrum analysis, with the significance of peaks tested against the corresponding red noise. For all the simulations, the zonal averaged time series were constructed over the monsoon sector (60-120E), Central Pacific (170E-130W) and the Eastern Pacific (110-50W), recorded at three latitudinal locations centred around 16N, the equator and 16S. The power spectra of the model zonal wind and precipitation for Expt.A (solid line) and Expt.B (dash line) are shown in *Figs 1.1.1a* and *1.1.1b* respectively. The corresponding red noise spectra are presented as lines with symbols. As can be seen from these figures, there is considerable power at several interannual frequencies, especially at 3-6 year period, for Expt.A. However, this interannual variability is generally insignificant (below red noise) when the interannual variability in SST is suppressed (Expt.B) implying that the interannual variability of mean winds alone is not sufficient for the genesis of low frequency variabilities. So we reach the first conclusion that convective internal dynamics can sustain low frequency climate variabilities in the presence of observed interannual variabilities of SST, without explicit ocean-atmosphere coupling.

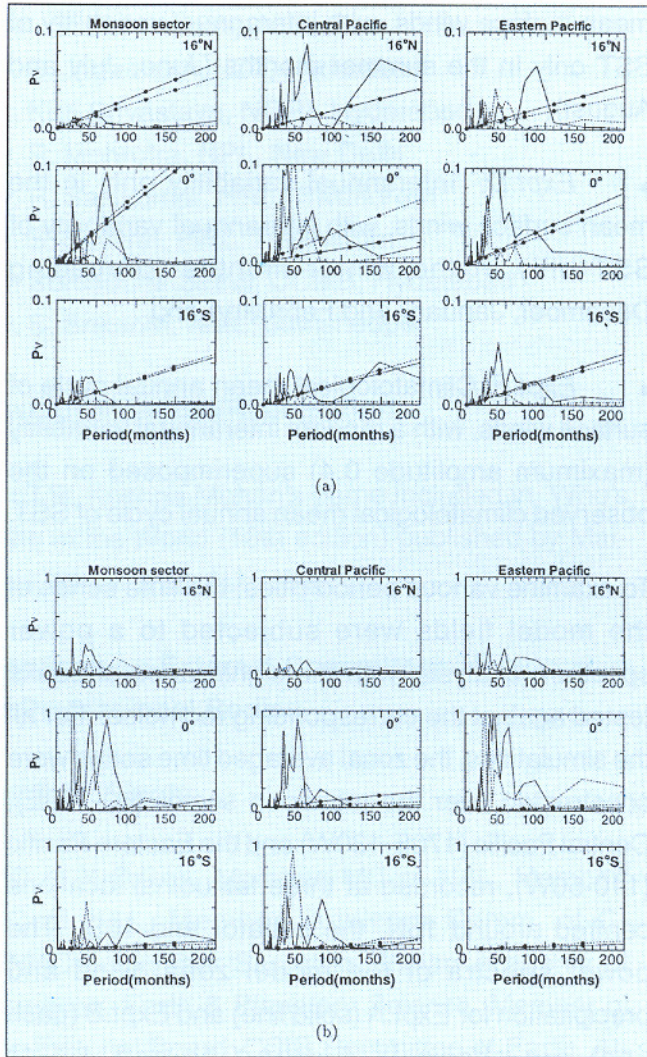


Fig. 1.1.1. Power spectra of time series of the model fields from long-term simulation with the observed interannual variability in both SST and the mean wind (Expt.A, solid line) and with observed interannual variability only in the mean wind (Expt.B, dash line). The relatively strong annual cycle has been removed by a 12-month running average. The ordinate is $vP(v)$ and abscissa the period. The red noise spectra are marked with symbols. (a) Zonal wind (b) Precipitation.

The role of the observed SST variability in the genesis of low frequency oscillations is addressed through Expt.C (solid line) and Expt.D (dash line). The results are presented as power spectra of the model zonal wind (Fig 1.1.2a) and precipitation (Fig 1.1.2b). While Expt.A and Expt.B demonstrate that an interannual variability of SST is necessary for the excitation of observed low frequencies, Expt.C

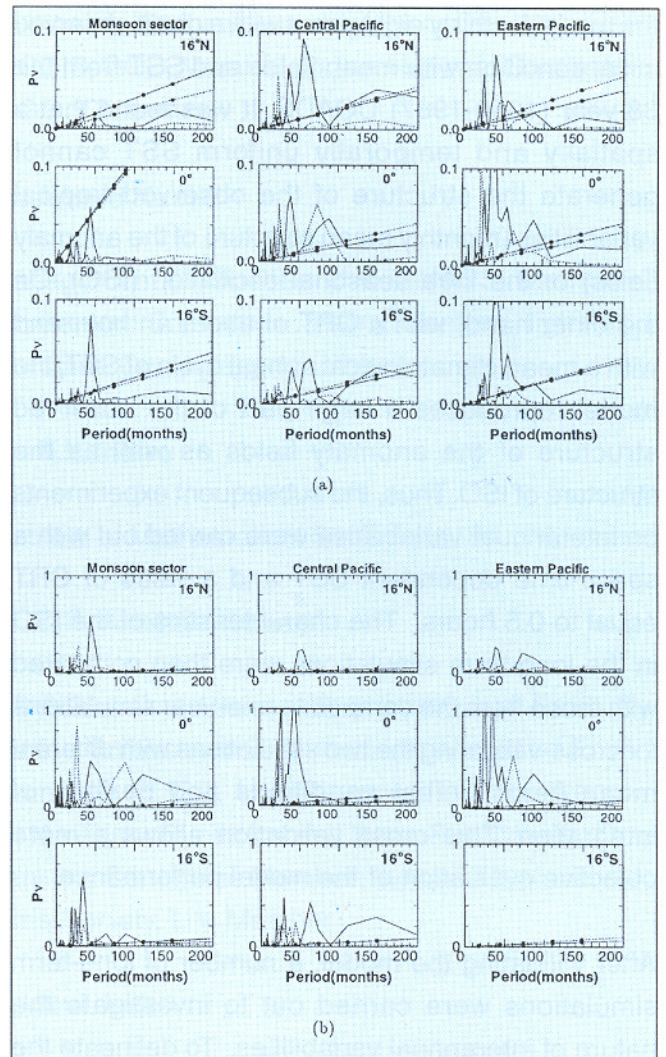


Fig. 1.1.2. Power spectra of time series of the model fields from long-term simulation with the climatological (38-year) mean annual cycles of SST and the mean wind with superimposed observed summer (June, July, August) interannual variability of SST (Expt.C, solid line) and observed winter (preceding December, January, February) interannual variability of SST (Expt.D, dash line). The relatively strong annual cycle has been removed by a 12-month running average. The ordinate is $vP(v)$ and abscissa the period. The red noise spectra are marked with symbols. (a) Zonal wind (b) Precipitation.

and Expt.D show that these can be realized even when only a part of the observed interannual variability of SST (summer or winter) is incorporated. This raises an important question as to whether it is at all necessary to invoke the interannual variability of SST to explain the observed characteristics. The results of Expt.E (Fig. 1.1.3), which show significant power at 3-7 year time scale

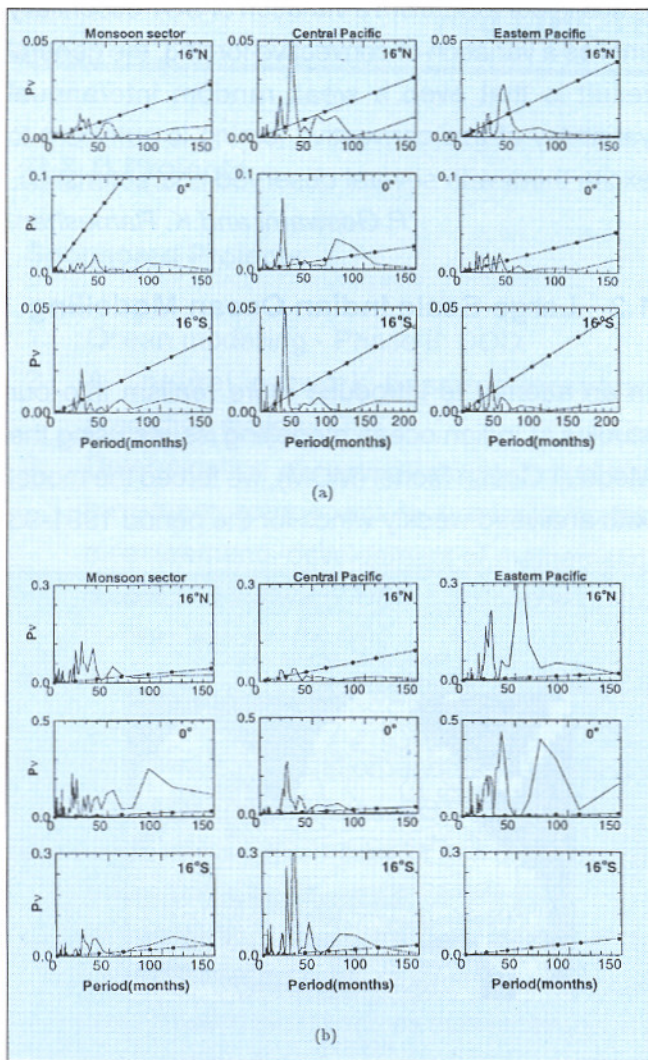


Fig. 1.1.3. Power spectra of time series of the model fields from long-term simulation with climatological (38-year) mean annual cycles of surface wind and SST, with a superimposed spatially and temporally uncorrelated random (maximum amplitude 0.4) interannual variability of SST (Expt.E). The relatively strong annual cycle has been removed by a 12-month running average. The ordinate is $vP(v)$ and abscissa the period. The red noise spectra are marked with symbols. (a) Zonal wind (b) Precipitation.

over a number of locations, demonstrate that even a weak random interannual variability of SST, representing spatially and temporally uncorrelated error (resulting either from observational error, or model error, or both) can support low frequency variabilities in the tropics.

It remains to be ascertained, however, that the model fields with these periodicities also possess

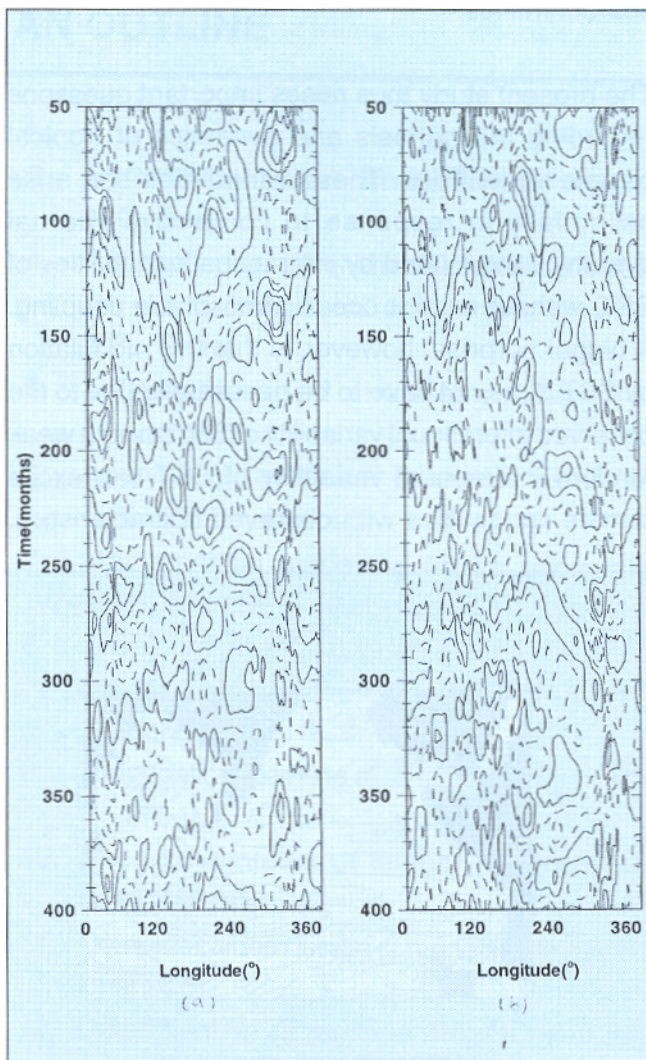


Fig. 1.1.4. Time-longitude structure of the model zonal wind over the equator from long-term simulations filtered for periods 48 to 72 month and spatially smoothed by a 10-point averaging. (a) with observed interannual variability in both wind and SST (Expt.A, left panels) and (b) with climatological (38-year) mean annual cycle of surface winds and a random interannual variability of SST (maximum amplitude 0.4) superimposed on the observed climatological (38-year) mean annual cycle of SST (Expt. E, right panels).

the other observed characteristics of ENSO-type variabilities. Fig. 1.1.4 shows the time-longitude structures of the zonal wind over the equator for Expt.A (1.1.4a) and Expt.E (1.1.4b) filtered at 3-7 years. It can be seen that the fields exhibit several observed characteristics of ENSO-type variabilities like the eastward propagation. It is interesting that, as in the observed fields, the model oscillations exhibit spatial and temporal variation of their

characteristics.

The present study thus raises important questions regarding the genesis and dynamics of tropical climate variabilities. These variabilities can arise essentially in response to convective internal dynamics modulated by interannual variabilities of SST, without explicit ocean-atmosphere coupling. A bigger surprise, however, is that this modulation by SST does not have to be necessarily due to the observed interannual variability of SST; even a weak random interannual variability of SST can excite climate variabilities with observed characteristics.

Since in our formalism a variation of SST essentially implies a variation of convective forcing, the general result is that even a weak random interannual variability of this convective forcing is sufficient to excite them with several observed characteristics.

(P. Goswami and K. Rameshan)

1.2 Large-Scale Indian Ocean Modelling

In an attempt to introduce more realism into our studies of Indian ocean modelling issues using the Modular Ocean Model (MOM), we forced the model with analysed weekly winds for the period 1991-93

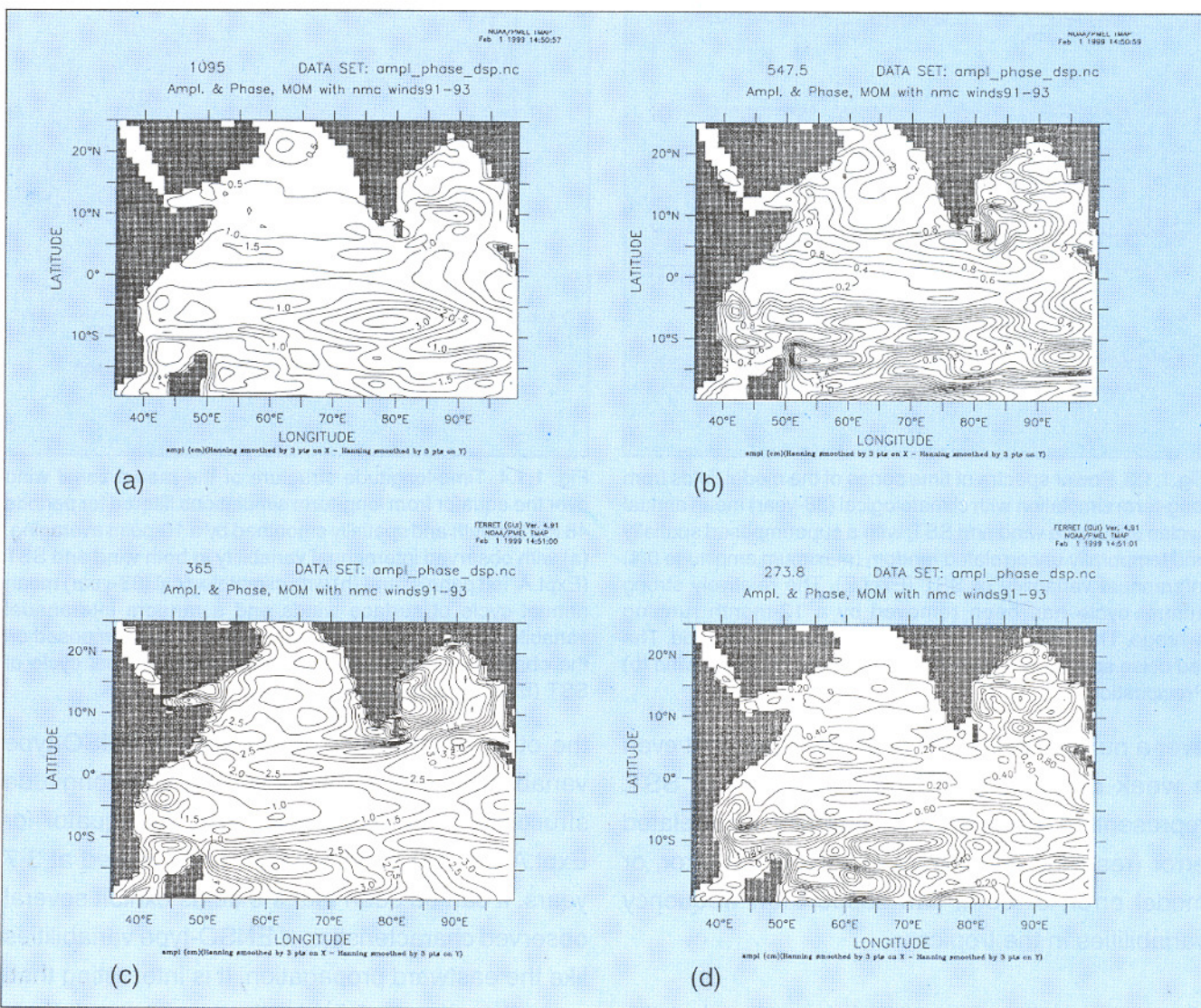


Fig. 1.2.1 Amplitude of the spectral components of sea surface heights for periods 1095-273 days.

obtained from National Met. Center (NMC), USA. The spatial resolution of the wind stress data is roughly 1.5 degrees in both latitude and longitude. This data on the surface was interpolated for the global MOM grid (362*273) of 1 degree resolution in the longitude and 1/3 degree in the latitude between 30S and 30N with increasing spacing towards the poles. The global run was integrated for 20 years with climatological forcing, with a time step of 45 minutes after which NMC winds were introduced into the model. The boundary conditions on heat and salt remained the restoring conditions with a space scale of 10 m and a time scale of 10

days. The model was integrated for 3 more years. In continuation of our earlier study where a comparison was made between sea surface heights (SSH) from MOM and those from Topex/Poseidon altimeter on a climatological scale, we investigated the variability of SSH over 3 years to isolate the temporal and spatial variability over the Indian Ocean. Data for SSH were output at 10 days intervals and an FFT over time was performed at each spatial location. The amplitude of the spectral components with periods ranging from 1095 days (3 years) to 273 days is shown in Fig. 1.2.1, from

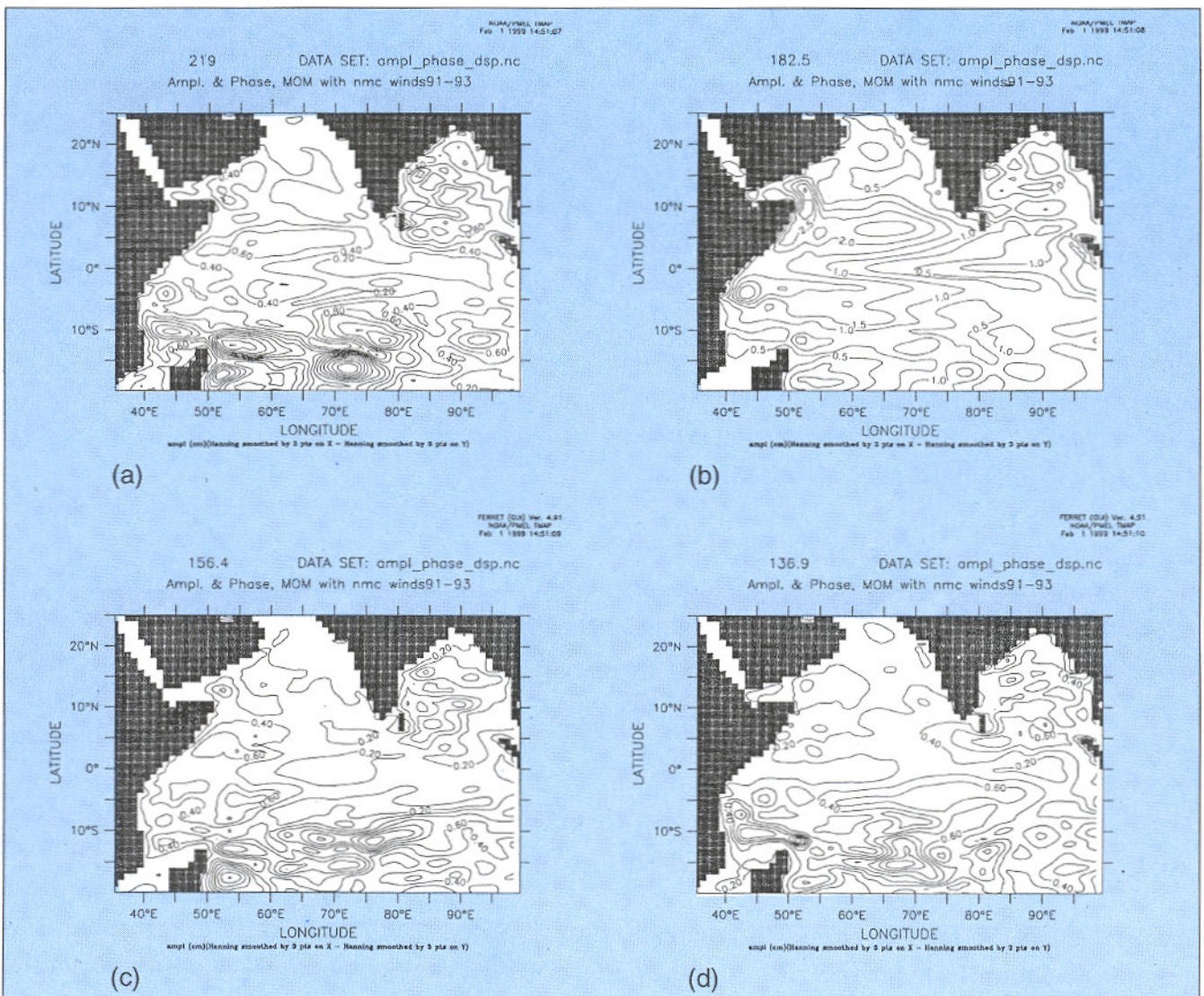


Fig. 1.2.2 Amplitude of the spectral components of sea surface heights for periods 219-136 days.

219 days to 136 days in *Fig. 1.2.2*, and 121 days to 91 days in *Fig. 1.2.3*. The spatial data for clearer illustration has been smoothed with a 3*3 Hanning filter. No filtering in time was done.

As expected, the largest amplitudes are found in the annual cycle (*Fig. 1.2.1c*) due to the Monsoon. The amplitude reaches almost 8 cm in the Bay of Bengal. There is also a strong signal as expected near the Somali region. Most of the Indian Ocean

shows a good annual signal. In addition, there are larger period signals (1095 days) in the Southern Indian Ocean south of 5S. These are attributed to the spectral variation in the NMC winds. Further, there is also a strong semi-annual signal (*Fig. 1.2.2b*) over most of the Indian Ocean with predominance in the southern Arabian Sea. The signals at other periods are comparatively weaker.

(P.S. Swathi)

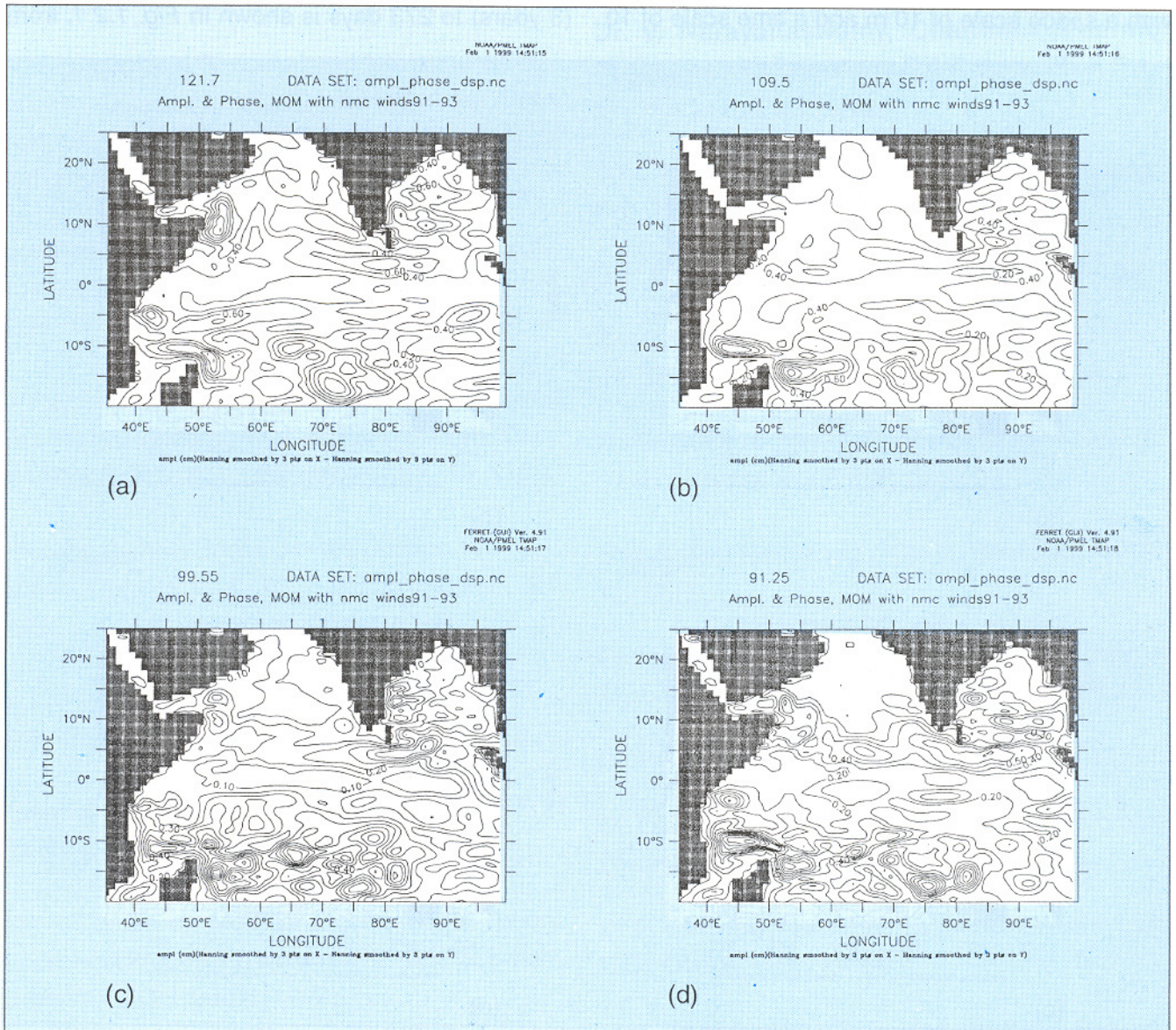


Fig. 1.2.3 Amplitude of the spectral components of sea surface heights for periods 121-91 days.

Lagrangian particle transport in the Arabian Sea and Bay of Bengal

In order to study the mixing characteristics due to the Monsoon reversal, we introduced 3000 particles in the southern Arabian Sea (66-70E, 6-10N and 0-400 m depth). The particles were introduced on Jan. 1, 1991, forced with NMC winds and tracked for 3 years. The particle positions after 1 year (Jan 1992) are shown in the left panels of *Fig. 1.2.4* and those after 3 years (Jan 1994) are shown in the right

panels. The spreading of the particle cloud is considerably complex due to the current reversals. There are two major routes of spreading; one associated with the Arabian Sea Gyre and the other directed towards the Bay of Bengal, reaching an almost area filling behaviour at the end of 3 years. It is interesting to note that not too many particles get transported to the northern Arabian Sea even after 3 years. From the vertical sections, it may be noted that there is a bulk downward motion of particles in the upper 100m after the passage of

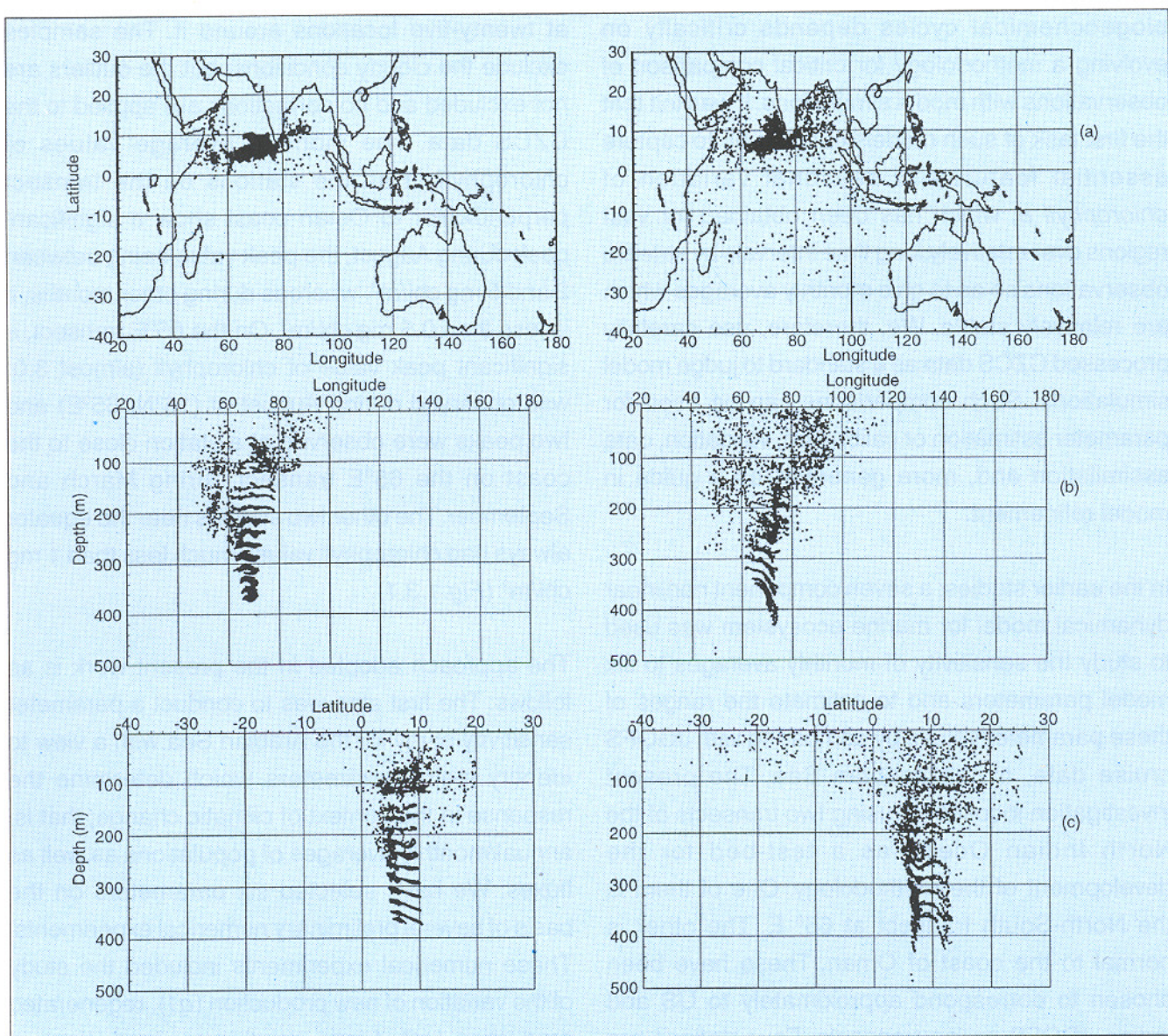


Fig. 1.2.4 Particle positions at the end of 1 year (Jan 1992, left panels) and at the end of 3 years (Jan 1994, right panels).

the first year. The deeper levels below 300m show little lateral mixing. A Liapunov-coefficient correlation-dimension analysis of the spreading rate has shown that the zonal dispersion is nearly diffusive and meridional is super diffusive.

(P. S. Swathi and Binson Joseph)

1.3 Ecosystem Modelling: Constraints from CZCS Data

The development of realistic models of biogeochemical cycles depends critically on evolving a methodology for critical comparison of observations with model simulations. It was felt that the first task of such models ought to be to capture essential features of seasonal variation of *chlorophyll a*, which has been obtained for vast regions over relatively long time intervals by satellite observations so as to give monthly averages which are relatively stable. We, therefore, use carefully processed CZCS data as a standard to judge model simulations. Such comparisons can be used for parameter estimation or calibration, validation, data assimilation and, more generally, as a guide in model refinement.

In the earlier studies, a seven component nonlinear dynamical model for marine ecosystem was used to study the sensitivity of monthly averages to six model parameters and to estimate the ranges of these parameter values by comparing with JGOFS cruise data, in the Arabian Sea. The present investigation focuses on using two transects of the North Indian Ocean as a test-bed for the development of the methodology. One of them is the North-South transect at 65° E. The other is normal to the coast of Oman. These have been chosen to correspond approximately to US and Indian JGOFS cruise transects. Four stations are chosen on the first transect at 0°, 8°, 16° and 24° N,

and four on the second at (18° N, 58° E), (17° N, 60° E), (16° N, 62° E) and (14.5° N, 65° E). The choice of only two transects is based on the view that model simulations should perform well at least on these transects, if they are to succeed in capturing the blooms in the north Indian Ocean, a major zone of marine productivity.

The monthly average values of chlorophyll is available from CZCS data at all the stations considered. The value of chlorophyll at a particular station is taken as the average value of chlorophyll at twenty-five locations around it. The samples exclude the cloudy conditions, but the outliers are not excluded and no corrections are applied to the CZCS data. The monthly average values of chlorophyll at all the stations on the transect perpendicular to Oman coast show a significant peak during August, the peak value being between 2 and 5 mg chl/m³, whereas during other months, it is less than 0.5 mg chl/m³. On the 65°E transect, a significant peak value of chlorophyll (almost 3.0) was observed during August at (16°N, 65°E) and two peaks were observed at a station close to the coast on the 65°E transect during March and September. The other two stations near the equator always had chlorophyll values much less than 1 mg chl/m³ (Fig.1.3.1).

The approach adopted in the present work is as follows: The first step was to conduct a parameter sensitivity study for the Arabian Sea with a view to identify major parameters which determine the response in the context of climatic change; that is, annual/monthly averages of populations as well as fluxes. We have selected six parameters on the basis of several preliminary numerical experiments. These numerical experiments included the study of the variation of new production (*q1*), regenerated production (*q2*), f-ratio, relative concentrations of ammonium and nitrate, zooplankton, microbial loop

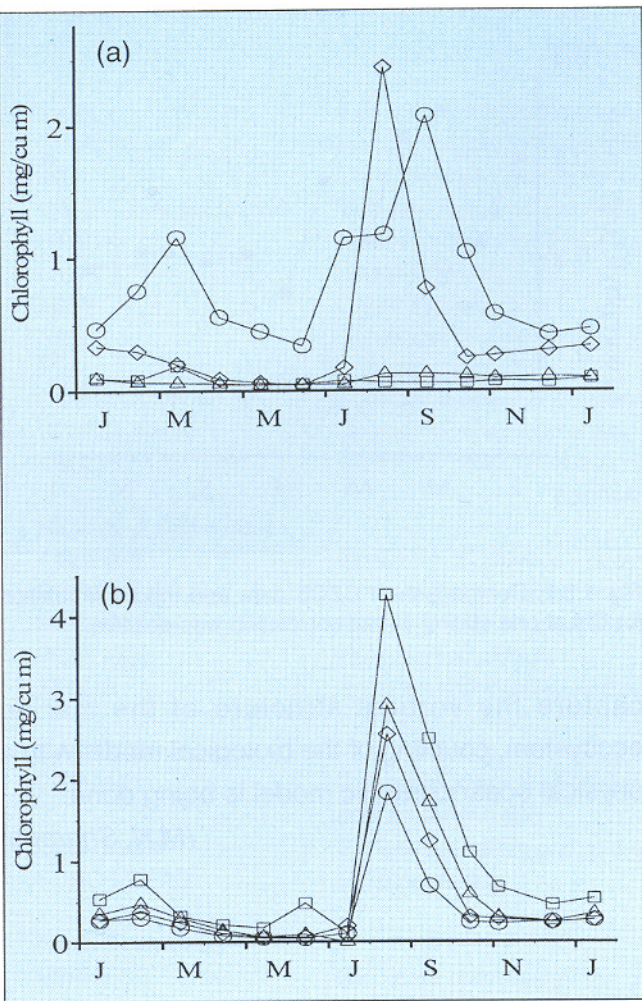


Fig. 1.3.1. CZCS data at stations (a) along 65 °E transect and (b) transect across Oman coast.

etc. These preliminary experiments showed that even with high concentrations of nitrate, regenerated production was more compared to new production, since ammonium is the more preferred food for phytoplankton. It can be seen from the simulations that if ammonium concentration is more than the half-saturation constant for uptake (0.5), q_2 will exceed q_1 . Also q_1 does not increase with increase in nitrate if nitrate exceeds 2.0 because of the model formulation and the values of half saturation coefficients, though ammonium is less. It was found that to increase the asymptotic value of q_1 , ammonium concentration should be decreased. The values for the rest were assumed on the basis of available literature. The threshold

for grazing on phytoplankton was introduced to get more realistic results. Earlier model studies at one station in Central Arabian Sea could not capture the bloom during August. To obtain the monthly average values of chlorophyll in the model simulation comparable to that of CZCS data, several modifications of the model formulation and model parameter values were tried. The software package to solve the seven component marine ecosystem model was modified to incorporate the effects of upwelling velocity, spatial variation of subsurface nitrate concentration, threshold for grazing on phytoplankton, self-grazing of zooplankton and nonlinear closure terms. Comparison of mean, standard deviation and correlation between model results and CZCS data was carried out for several numerical simulations - by varying grazing rate, mixing coefficient, detritus sinking velocity, grazing preferences, upwelling velocity, photosynthetically active radiation and subsurface nitrate concentration.

CZCS data show a significant peak in the monthly mean value of chlorophyll during July-August almost everywhere in the Indian Ocean. In the model, the peak value of chlorophyll was very much less compared to the data. The terms in the equation responsible for growth of phytoplankton were examined in more detail. Zooplankton mortality terms which were linear were replaced by a sum of linear and nonlinear terms.

Since the results of moderately large number of simulations are being assessed, several measures as indices of agreement have been considered like comparison between the mean of observations and simulations, squared deviation of the simulations from observations, the ratio of simulation results to observations, correlation coefficient between results of simulations and observed values. The model simulations having positive correlation with CZCS

data were studied in detail. The correlation coefficient was positive for two stations on the second transect when upwelling velocity, and photosynthetically active radiation were introduced. At these stations, the monthly averages of chlorophyll were high compared to CZCS data (Fig.1.3.2). All the model simulations showed two significant peaks during one year period whereas CZCS data showed only one significant peak. The peak value of chlorophyll during summer months may be due to the model formulation which does not contain terms describing horizontal advection.

To get more realistic results, some modifications in the model formulation and fine tuning of parameters will be done. Models describing the complete food web from primary production to fisheries potential are being studied. Also, simple models of the marine ecosystem are being studied in detail to understand the nonlinear dynamical behaviour. Further, to

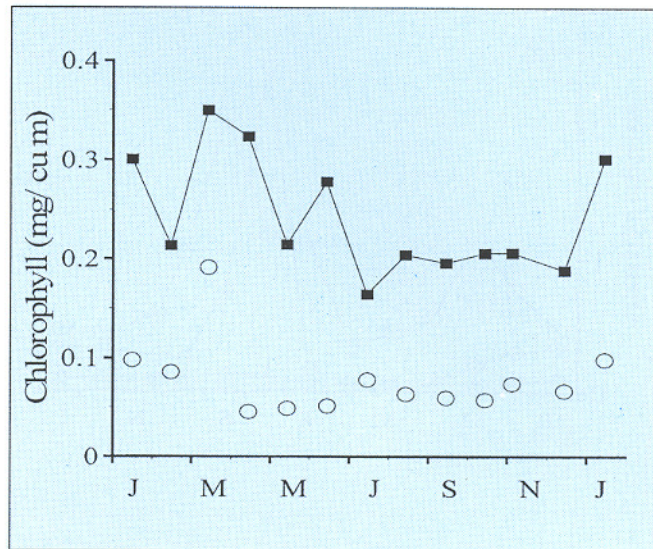


Fig. 1.3.2. Comparison of CZCS data and model simulation for Chl at one station where correlation was positive.

capture the vertical structure of the marine ecosystem, coupling of the biological model with a physical oceanographic model is being done.

(M.K. Sharada)